Strain-induced crystallisation of reinforced elastomers using surface calorimetry

Jean-Benoit Le Cam, William Amoako Kyei-Manu, Adel Tayeb, Pierre-antoine Albouy, James J.C. Busfield

Polymer Testing 131 (2024) 108341

Contents lists available at ScienceDirect

Polymer Testing

journal homepage: www.elsevier.com/locate/polytest

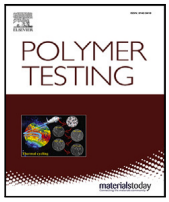

Strain-induced crystallisation of reinforced elastomers using surface calorimetry

Jean-Benoit Le Cam [a,*], William Amoako Kyei-Manu [b], Adel Tayeb [a], Pierre-Antoine Albouy [c], James J.C. Busfield [b]

[a] Université de Rennes, Institut de Physique de Rennes, UMR 6251 CNRS/Université de Rennes, Campus de Beaulieu, Bât. 10B, 35042 Rennes Cedex, France
[b] School of Engineering and Materials Science, Queen Mary University of London, London E1 4NS, UK
[c] Laboratoire de Physique des Solides, CNRS, Université Paris-Sud, Université Paris-Saclay, 91405 Orsay, France

ARTICLE INFO

Keywords:
Strain-induced crystallinity
Carbon black
Natural rubber
Surface calorimetry
X-ray diffraction
Entropic effects

ABSTRACT

The crystallinity of rubbers which are amenable to crystallisation upon stretching is classically measured using X-ray diffraction (XRD) techniques. Recently, an alternative method for evaluating the crystallinity in unfilled natural rubber (NR) during stretching was proposed. This method is based on surface calorimetry principles (Le Cam, 2018) and was validated by XRD measurements in Le Cam et al. (2018). For reinforced rubber composites, the calorimetric response is not only due to the elastic couplings and the crystallisation/melting process, but also due to the intrinsic dissipation and additional viscoelastic dissipation resulting from the presence of fillers. This makes estimating the crystallinity of carbon black (CB) reinforced rubber compounds from calorimetric techniques typically more challenging. In this paper, however, the calorimetric approach for measuring crystallinity for CB reinforced rubber compounds was investigated. Crystallinity measurements were performed using both an unfilled and three CB reinforced NR compounds. A comparative study was performed using the XRD technique on the same four compounds. The results confirmed the appropriateness of the calorimetric technique for determining the crystallinity in the unfilled NR. The combination of the XRD and the calorimetric techniques allowed the different heat sources under strain to be identified and therefore, the thermal energy associated with crystallisation to be determined. This was done initially using one of the CB reinforced NR compounds and validated using the two other CB reinforced NR compounds. The results show reasonable correlation between the crystallinity measured using the novel calorimetric technique and the classical XRD technique for CB reinforced NR compounds. The development of this methodology has potentially significant impact. The calorimetric approach does not require the measurement of the mechanical response during testing. This is useful for measuring crystallinity gradients from infrared thermography coupled with full kinematic field measurements, typically at crack tips, where estimating the local mechanical response is very difficult or inaccurate.

1. Introduction

The first publications on crystallisation in natural rubber (NR) dates back to the 1920s. In 1925, Feuchter observed that the volume of NR decreased with elongation and attributed this observation to the formation of an anisotropic system in stretched NR. In the same year, the pioneering work by Katz [2] provided the first X-ray diffraction (XRD) pattern of stretched NR. The subsequent studies on NR, investigated the role of the crystallisation on its fatigue properties. NR was shown to be more resistant to fatigue damage compared to non-crystallising rubbers [3–5]. The high fatigue resistance of NR was attributed to strain-induced crystallisation (SIC) effects, although the exact mechanisms for enhancing lifetime had not been fully identified. This motivated studies using the XRD technique to understand SIC phenomenon including the crystalline phase structure [6–9], chain orientation [10], and kinetics of crystallisation [11,12]. XRD has therefore been an essential technique for elucidating our understanding of SIC in rubber materials. Brüning et al. measured the crystallinity around the crack tip under dynamic loading conditions using Wide Angle X-ray diffraction (WAXD) and discovered that the crystallinity is significantly reduced compared to scans at the crack tip under static loading conditions [13]. Rublon et al. also coupled digital image correlation (DIC) and X-ray diffraction to determine a link between volume of the crystallised zone and fatigue crack growth rates [14]. The

* Corresponding author.
E-mail address: jean-benoit.lecam@univ-rennes1.fr (J.-B. Le Cam).

https://doi.org/10.1016/j.polymertesting.2024.108341
Received 12 October 2023; Received in revised form 9 January 2024; Accepted 14 January 2024
Available online 19 January 2024

use of X-rays in a laboratory, however, poses certain challenges. For example, it requires compliance to specific layouts of the test laboratory and regulatory constraints such as requiring a person competent in radiation protection and isolation of X-ray installations within the laboratory. This is however not the case for infrared thermography and more generally, temperature measurements. Very few requirements mostly related to experimental set up such as limiting external IR radiations and ensuring that the camera is positioned perpendicular to the surface being observed are needed in using the thermal camera to measure crystallinity. As such, it can be adapted to a wide range of testing machines in a lab.

SIC is strongly exothermic and thus, there is a noticeable increase in temperature when it occurs. Since Mitchell and Meier pioneered using temperature measurements to estimate crystallinity [15], several researchers have followed suit and used different evaluation techniques to estimate crystallinity from temperature measurements. Candau et al. used thermal and mechanical measurements to determine the onset of crystallisation at different strain rates and found relatively good correlation between the two measurements [16]. Plagge and Klüppel used an energy balance approach to determine the crystallinity of different types of unfilled and filled NR compounds [17]. They found a transition from triangular-shape crystallinity to tube-like curves, which was interpreted as the effect of differently amplified domains by the authors. In this paper, the calorimetric response is used to determine crystallinity. A methodology for evaluating the crystallinity in unfilled NR from surface calorimetry was recently developed by Le Cam [18] and validated by comparing the results obtained using the calorimetric technique with the results obtained using the classical XRD technique on the same material [19]. Crystallinity measurements by surface calorimetry is an accessible technique that does not require the measurement of the mechanical response which makes it much more useful in practice. The method allows the crystallinity to be determined while stretching the sample. However since the calorimetric response while stretching is used to determine the crystallinity, there is no requirement to measure the force during stretching. In most engineering applications, the elastomers used are reinforced with fillers such as carbon black (CB), and thus it is necessary to extend the crystallinity measurement from surface calorimetry to CB reinforced elastomers as well. This could have significant applications such as mapping the crystallinity field at crack tips in CB reinforced elastomers. Even though calorimetric measurements have already been performed for reinforced rubbers [20–24], the crystallinity was not evaluated from these measurements. The aim of this study is to extend the measurement of the crystallinity from the calorimetric response to CB reinforced rubber compounds during stretching. The XRD technique was used to develop the methodology for measuring crystallinity from the calorimetric response using 3 CB reinforced NR compounds and as far as the authors are aware, this represents the first direct comparison of the crystallinity from thermography and XRD measurements on the same set of compounds under similar loading conditions. Section 2.1 discusses the two techniques used to determine the crystallinity during rubber deformation. Section 3 provides detailed materials data including the compound formulation, CB types and their properties and sample geometry used for the measurements. The section also discusses the loading conditions of the surface calorimetry tests. In Section 4, the surface calorimetry technique is initially applied to the unfilled NR and the results are compared to the results from the XRD measurements. The surface calorimetry technique is then generalised to CB reinforced compounds using one of the CB reinforced NR compounds. The methodology is developed by comparing the results with the XRD measurements made under similar strain conditions on the same compound. The proposed methodology is then validated by applying it to the two other CB reinforced NR compounds and the results are compared to the crystallinity obtained from the XRD measurements of these compounds.

2. Experimental techniques for evaluating the strain-induced crystallinity

2.1. X-ray diffraction

Crystallinity indices provided here are derived from an analysis of angular scans centred on the amorphous halo. The methodology adopted follows the procedure detailed in [25]. This method combines simplicity and direct access to the Herman orientation parameter for the amorphous phase. Other parameters provided by this XRD technique include the crystallite dimensions and their orientation with respect to the extension axis. In this study, a uniaxial tensile testing machine was installed on a rotating anode generator operated at medium power (copper anode, 40 kV, 40 mA, focus size: 0.2×0.2 mm^2). The uniaxial tensile testing machine was a custom-built machine as detailed in previous publications such as [19,26] which discuss the XRD technique. The CuK_α radiation is selected with a doubly curved graphite monochromator and the sample is located at the focal point which ensures optimised diffracted intensity. The set-up is equipped with a hybrid pixel detector that combines high efficiency with low signal to noise ratio. The crosshead extension can be varied between 1 mm/min and 800 mm/min. However, since it was necessary to collect a sufficient number of frames (acquisition time: 0.2 s) during the stretching phase, the maximum extension rate was limited. The incident beam diameter was ca. 1 mm, which precluded any detailed analysis of heterogeneous zones, if any. The crystallinity is determined from the X-ray measurements following classical steps detailed in literature such as [27,28]. The chosen scans capture the intensity scattered by the first most intense diffraction spots and by the so-called amorphous halo. We verified that the total intensity scattered within this angular range remains nearly constant (±3%). It is thus expected that the crystallinity index defined this way is close to the actual crystallinity.

2.2. Surface calorimetry from infrared (IR) thermography

Most mechanical tests are conducted under non-adiabatic conditions. The temperature measured is therefore affected by heat diffusion between the sample and environment. Measured temperature changes are therefore not solely due to the material deformation and cannot be used directly to determine the crystallinity or onset of SIC. To overcome this issue, the heat diffusion equation is used to determine the corresponding heat source from the temperature measurement. The heat source, or the heat power density, provides the calorimetric response and is intrinsic to the material deformation processes. The heat source field is considered to be homogeneous (the heat conduction through the sample plane is neglected) and any temperature gradient in the sample's thickness is ignored. The sample therefore has to be relatively thin (see details in [29] and in [30] which show the heat source calculation applied to the case of rubber). Under such conditions, the tri-dimensional formulation of the heat diffusion equation which is discussed in detail in [18] can be simplified as follows (see details in [31]):

$$\rho C \left(\dot{\theta} + \frac{\theta}{\tau}\right) = S \tag{1}$$

where S is the heat source or heat power density and θ denotes the temperature variation with respect to the equilibrium temperature T^{ref} in the reference state. T^{ref} corresponds to the undeformed state and is constant and equal to the ambient temperature. Under conditions where changes in ambient temperature occur, T^{ref} has to be corrected accordingly with the measurement of ambient temperature variations. ρ and C are the material's density (in kg/dm^3) and the specific heat capacity (in J/(kg K)) respectively. For the purpose of this study, the density is assumed to be independent of strain and temperature. The specific heat capacity varies with temperature for the heat source calculations. The heat exchange through convection with air at the

surface of the samples is characterised by the heat exchange parameter, τ. As discussed by [32], τ is defined as:

$$\tau = \frac{e\rho C}{2h} \tag{2}$$

where e is the sample thickness, h is the convection coefficient, ρ is the material's density and C is the specific heat capacity. In practice, τ can be experimentally determined by identification from the natural return to ambient temperature after the sample is homogeneously heated (or cooled) for a specific testing configuration. During the return to ambient temperature, the heat source is equal to zero. Consequently, the only unknown in Eq. (1) is τ leading to

$$\theta(t) = \theta_0 e^{-\frac{t}{\tau}} \tag{3}$$

where θ_0 is the temperature change at $t = 0$ s. When the thickness changes significantly, which is the case during large deformation, the heat exchange coefficient has to be compensated for accordingly. For large deformations, τ therefore depends on the stretch, λ and is either determined by measuring it at different increasing stretches (further details are given in [33]), or corrected according to its dependency on the stretch for the case of an incompressible material. If τ is determined by measuring it at different increasing stretches, the value during the natural return to ambient temperature for stretches greater than the onset of crystallisation is affected by additional heat produced (absorbed) by the crystallisation (melting) during the material cooling (heating). As such for this study, $\tau(\lambda)$ was determined from its value in the undeformed state (denoted as τ_0) and adjusted based on the link between the thickness of the specimen and the stretch. When the material is incompressible, the thickness varies proportionally with $\frac{1}{\sqrt{\lambda}}$ and τ becomes for the case of uniaxial tension:

$$\tau(\lambda) = \frac{\tau_0}{\sqrt{\lambda}} \tag{4}$$

Tau measurements at different elongations and at different bi-axial ratios were performed in [30] with an unfilled nitrile rubber compound. The measured values provided good correlation with the predicted values when the material was assumed to be an incompressible material. From the simplified formulation of the heat diffusion equation, the crystallinity can be evaluated from the part of the total heat source that is produced by SIC only, which gives access to the crystallisation temperature T_{cryst}. The crystallinity χ can then be deduced from T_{cryst} by considering that the crystallisation energy can be approximated by the enthalpy of fusion ΔH (in J/dm^3) [18,34]:

$$\chi(t) = \frac{\rho C T_{cryst}(t)}{\Delta H} \tag{5}$$

For reinforced rubber compounds, this ratio is weighted by the factor $\frac{1}{1-\Phi_{filler}}$, where Φ is the filler volume fraction (which is the volume fraction of the elastomer composite that cannot crystallise). Practically, the methodology for determining the crystallinity can be summed-up by the diagram in Fig. 1. It comprises four steps:

- ***Step*** *1:* The heat source is calculated by applying Eq. (1). It requires the temperature variation θ, τ parameter and the thermophysical parameters ρ, C and ΔH. The typical increase in the heat source produced in unfilled NR once crystallisation starts [33,35] is shown in the figure. λ_c stands for the stretch at which SIC starts. It should be noted that the heating effects accompanying SIC cannot be separated from dissipative heating of the rubber material. However, it is possible to separate the heating effects accompanying SIC from the heating effects due to both thermoelasticity and the intrinsic dissipation. And this is the main objective of the present paper when choosing the functions to predict the heat source due to both thermoelasticity and the intrinsic dissipation before SIC occurs. The good correlation found between the crystallinity measured by XRD and surface calorimetry helps to validate this approach. The ability of the XRD technique to directly provide the crystallinity is indeed an advantage, especially at the crack tip as discussed in [36–38].

Table 1
Compound formulation.

Component	Loading/phr
NR-SMR CV-60	100
Carbon Black	50
Zinc Oxide	5
Stearic Acid	3
Anti-ozonant/Antioxidant	3
Micro-wax	2
Sulphur	2.5
TBBS[a]-75	0.8

[a] N-Tertiarybutyl-2-benzothiazolesulfenamide, 75% assay.

- ***Step*** *2:* The thermal energy due to SIC is deduced from the area located between the measured heat source (curve A) and the part of the heat source that would be due to the elastic couplings only (curve B). The latter is predicted by using a function, whose parameters are identified by fitting the heat source measured before SIC starts ($\lambda < \lambda_c$). The choice of the function is discussed in detail in Section 4. Step 2 shows the forms of the three functions that are considered in this paper.
- ***Step*** *3:* The crystallisation temperature, T_{cryst}, is calculated from the heat source due to SIC using the numerical scheme in step 3. The heat source due to SIC is given as the area between curves A and B.
- ***Step*** *4:* The crystallinity then is calculated using Eq. (5).

This method is simple and does not require measuring the nominal stress nor the characterisation of other non-entropic effects [39,40] because they are included in the calorimetric response. A main benefit of the calorimetric approach is that the heat source produced by SIC can be directly linked with constitutive equations through the thermomechanical couplings (as described in [41]). Although this technique does not provide information on the crystalline phase structure and chain orientation, it provides important information on the nature of elasticity in elastomers, due to entropic and/or isentropic coupling [33,40,42,43]. It also enables the identification of the mean intrinsic dissipation due to viscosity and damage [20,21,24], and to map the crystallinity field from the temperature measurement using an IR camera.

3. Experiments

3.1. Material and sample geometry

To extend the crystallinity measurement using the surface calorimetry technique to CB reinforced rubbers, one unfilled and three CB reinforced NR compounds were used. The reinforced compounds had the same filler loading of 50 parts per hundred rubber in weight (phr). The CBs used varied in their structure and surface area which was the only difference between the compounds. An unfilled equivalent compound was also tested to reproduce the calorimetric technique for measuring SIC.

The formulation of the compounds is provided in Table 1. Table 2 shows the structure and surface area of the three CB grades as measured using compressed oil absorption number (COAN) and statistical thickness surface area (STSA) respectively. The type of CB influences the dynamic and static mechanical properties of the resulting compound. The N326 compound, with a comparatively higher CB structure, has a higher incremental modulus at medium to high strains compared to the R1200 and R2000 compounds due to matrix overstrain effects [44]. Table 2 also shows the density of the compounds. The density was calculated using the mass in air and mass in isopropanol (density = 0.787 g/cm^{-3}) measured using an Adam Equipments density balance.

The compounds were prepared in Birla Carbon (Marietta GA, USA) using a 1.6 L capacity Banbury mixer. The samples were mixed using a 3-stage mixing procedure as detailed in the supplementary section.

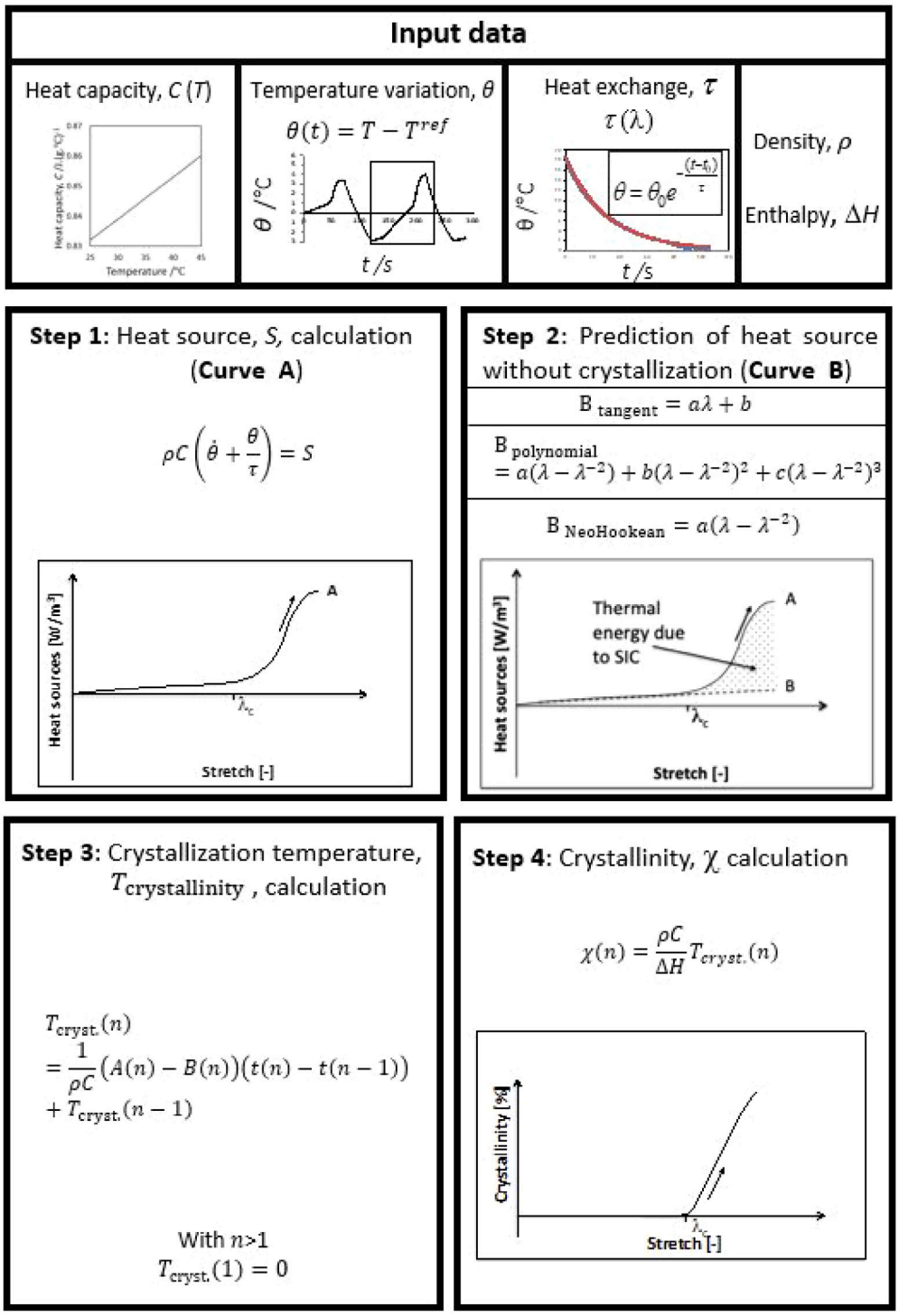

Fig. 1. Methodology for determining crystallinity from temperature variation measurement.

Table 2
CB morphological properties and corresponding compound density.

Carbon black/ compound	Structure (COAN)/cc.(100 g)$^{-1}$	Surface area (STSA) /m^2 g^{-1}	Density kg dm^{-3}
N326	73	76	1.130
R2000	62	161	1.136
R1200	55	96	1.135
Unfilled NR	NA	NA	0.971

The T_{90} of the samples at 150 °C were measured using a moving die rheometer (MDR) from Alpha Technologies. Vulcanised sheets measuring 110 mm × 110 mm × 2 mm were prepared via compression moulding at 150 °C for a time of T_{90} + 5 min. For both the surface calorimetry tests, strips measuring approximately 40 mm × 5 mm × 2 mm in gauge length, width and thickness respectively were cut from the vulcanised sheets so that the longitudinal axis was in the milling direction.

Fig. 2 shows the normalised heat capacity of the compounds as a function of temperature from 25 °C to 40 °C. The heat capacity was

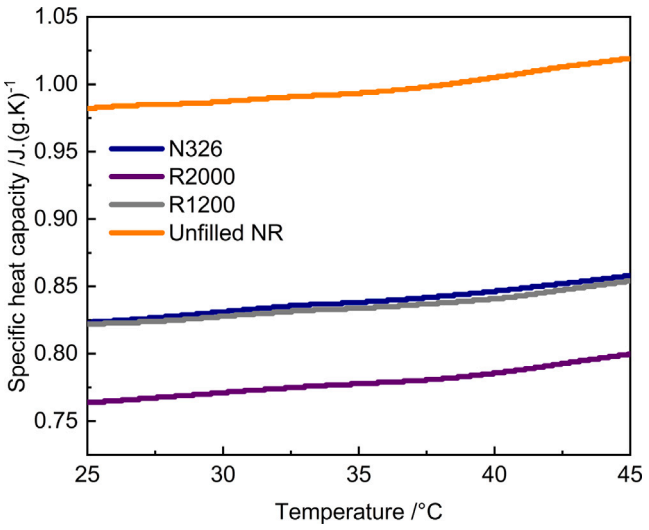

Fig. 2. Heat capacity as a function of temperature for tested compounds.

measured using a TA Instruments Differential Scanning Calorimeter (DSC) 25 using a modulated heat ramp at a rate of 3 °C/min. The specific heat capacity varies between approximately 0.75 J/(gK) to 1.00 J/(gK) depending on the compound and slightly increases with temperature.

3.2. Loading conditions

The unfilled NR compound was cycled 5 times at a maximum stretch of 6 while for the CB reinforced NR compounds, 5 cycles were applied at each increasing maximum stretch of 2, 3, 4, 5 and 6. All the tests were conducted at a loading rate of 300 mm/min which equates to a target strain rate of 0.125 /s. In this paper, only the fifth cycle of the last set of cycles at the prescribed maximum stretch ($\lambda = 6$) have been used for analysis. This represents the thermodynamical cycle and are referred to as the last mechanical cycle in this paper. This is a constraint imposed by the calorimetry technique as discussed in [45]. The analysis for the XRD measurements was also performed on the same cycle for comparison. The previous cycles were performed to investigate the calorimetric response and the dissipative nature of materials versus the cycle number for future analysis. It is worth highlighting that the stretch is recalculated at each cycle in order to account for any residual stretch developed in the cycle prior to the last one. It is assumed that at each new cycle, the residual stretch increases the unstrained length. As a result of this, for both the unfilled and CB reinforced compounds, the value of the stretch used in presenting the results (which is denoted as corrected stretch in the graphs), is always lower than the one that was targeted during the measurement. Fig. 3 shows the gripping of the samples in the jaws for the surface calorimetry measurements. The figure shows the samples were wound around a metal axle with high-roughness double-sided sandpaper placed between the samples and the jaw. To validate the evaluation of the crystallinity with the surface calorimetry technique, the crystallinity was also determined from XRD measurements with a different device but using broadly similar loading conditions.

3.3. Thermal measurements

Temperature measurement was performed using a cooled high-resolution FLIR X6540sc infrared camera equipped with a focal plane array of 640 × 512 pixels and detectors operating in wavelengths between 1.5 and 5.1 μm. The acquisition frequency was equal to 10 Hz. The calibration of camera detectors was performed with a black body using a one-point NUC procedure at this acquisition frequency. The thermal resolution, which refers to the noise equivalent temperature difference (NETD), was equal to 20 mK for a temperature range between 5 and 40 °C. The infrared camera was switched on several hours before the test to stabilise its internal temperature. The surface emissivity was set at 0.94, according to the measurements on a similar material in [30].

4. Results

The results of the surface calorimetry technique applied to the unfilled NR compound are considered first and the calculated crystallinity is compared with that obtained using the XRD technique. The surface calorimetry methodology is developed and extended to CB reinforced rubber compounds using one of the CB reinforced NR compounds (R2000). To extend the methodology to the crystallinity measurement in CB reinforced NR compounds, the results from crystallinity measurements using XRD measurements are used to calibrate the surface calorimetry. The proposed methodology is validated by applying it to the two other CB reinforced NR compounds (R1200 and N326) and compared with the calculated crystallinity obtained using the XRD measurements.

4.1. Crystallinity in the unfilled (reference) NR and extension of the methodology to CB reinforced NR

Fig. 4 shows the mechanical response for the last cycle of the unfilled NR compound. It shows the nominal stress defined as the force per unit initial cross-sectional area as a function of the corrected stretch. The graph shows the classical hysteresis between the loading and unloading cycle presented previously in literature such as [11,46–48]. With no fillers included, the stabilised hysteresis loop is primarily due to the difference in kinetics of crystallisation and crystal melting and not from viscosity. In other words, no significant intrinsic dissipation is produced during the stabilised cycle as demonstrated in [33,40]. Fig. 5 shows the measured temperature variation (θ) as a function of time in solid black line. The mean temperature which is taken as the midpoint between the maximum and minimum values of the temperature decreased and stabilised at a value greater than zero. For example, the maximum and minimum temperatures on the fifth cycle in the graph are approximately 4.8 °C and −2.4 °C respectively and the mean temperature is therefore about 1.2 °C. This is attributed to the entropic coupling and not to the production of intrinsic dissipation as explained in [49]. The heat source in an elastomer depends on both the strain rate and the strain itself as the stress–strain relationship is not linear. This makes the temperature variation oscillate around a value greater than zero. It should be noted that during the loading cycles, the slope of the curve increased at the onset of crystallisation. In the special case where the measurements could be performed under adiabatic conditions, the onset of crystallisation could therefore be determined from the temperature variation. This was however not the case here and the heat source had to be calculated to determine the onset of crystallisation. The dashed black like in Fig. 5 shows the temperature variation if the test was performed under adiabatic conditions. It is calculated by integrating Eq. (1) over time without the diffusion term: $\theta_{adiabatic} = \int \frac{S}{\rho C}\, dt$.

To determine the heat source, the heat exchange parameter in the undeformed state, τ_0, is used. The specimen was heated in an oven at 50 °C for approximately 15 mins. The specimen was taken out and the decrease in temperature as it returns to ambient temperature is used to calculate τ_0 as shown in the input data section of Fig. 1. The dependency of the heat exchange parameter on the stretch is obtained by applying Eq. (4). When the material is assumed to have no intrinsic dissipation after stabilisation, it is possible to validate the calculation of τ by calculating the corresponding adiabatic temperature variation from the heat source. This appears as the black dashed line in

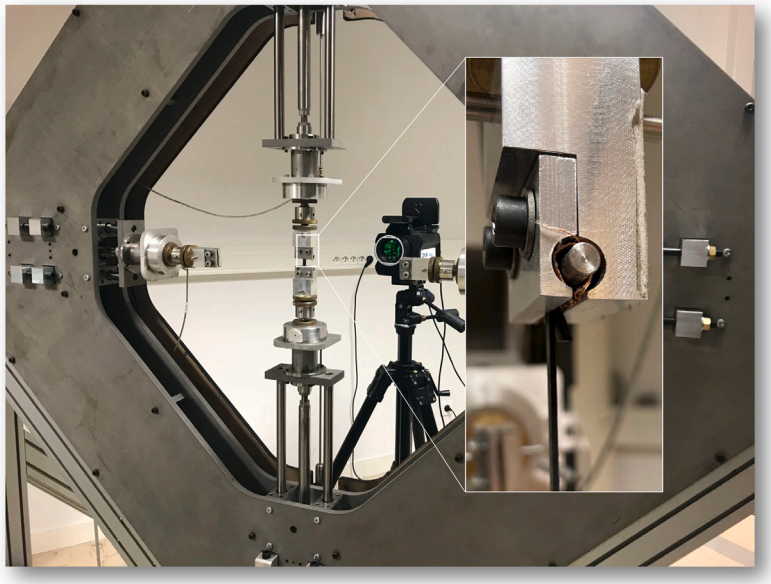

Fig. 3. Experimental device and sample gripping into the jaws.

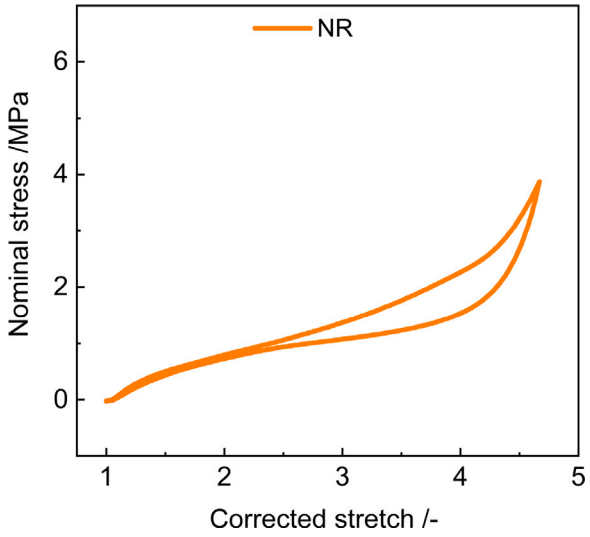

Fig. 4. Nominal stress versus corrected stretch for the last mechanical cycle of the unfilled NR.

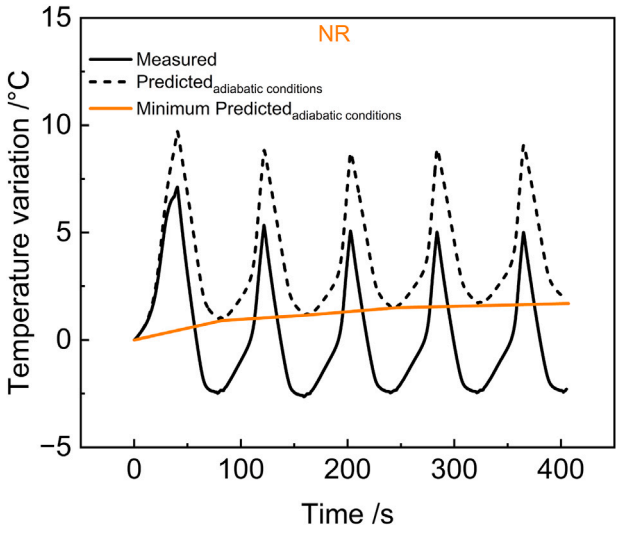

Fig. 5. Temperature variation versus time of the unfilled NR.

Fig. 5. There is a slight intrinsic dissipation during the first two cycles which could be attributed to effects such as the reorganisation of the macro-molecular network, the viscoelasticity in the rubber matrix, disentanglements and the breakdown of the filler network. It is difficult to de-convolute these different effects using our technique though. However following these two cycles, there was no further measurable intrinsic dissipation. The minimum temperature variation first increases during the initial cycles and then stabilises as traced by the orange line which passes through the minimum predicted temperature variation values under adiabatic conditions. This observation corresponds to the observation of a slight residual stretch after the first and second cycles in the mechanical response during testing. These observations confirm that τ has been well calculated.

Fig. 6 shows the power densities. The power densities refer to the heat power density obtained from the temperature measurements and the strain power density. The strain power density was calculated as $\pi\dot{\lambda}$. where π is the Piola–Kirchhoff stress tensor and $\dot{\lambda}$ is the stretch rate. The measured heat source (solid black line) and predicted heat sources (dashed lines) for the fifth cycle, which is considered a thermodynamical cycle (that is, the strain and temperature between the beginning and the end of the cycle are the same). As previously mentioned, the prediction of the heat sources is done to find the calorimetric response due to elastic couplings only. Three different possibilities have been considered for fitting the heat source before crystallisation occurs (which is before the significant increase in the heat produced). These are a tangent to the heat source (shown in green dashed lines), a Neo-Hookean form previously detailed in [49] (shown in blue dashed lines) and a third order polynomial (shown in purple dashed lines). It is worth pointing out that these fitting functions are only formal mathematical expressions. There are a couple of remarks worth highlighting with regards to the predicted heat sources:

Remark 1:. The Neo-Hookean and the third order polynomial expressions are proportional to the stretch rate. The predicted tangent fit

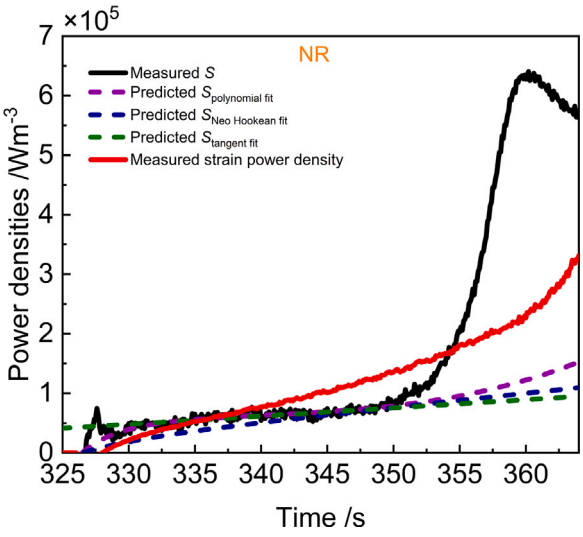

Fig. 6. Power densities versus time for unfilled NR on the fifth cycle. The time axis starts from 325 s since it shows the elapsed time.

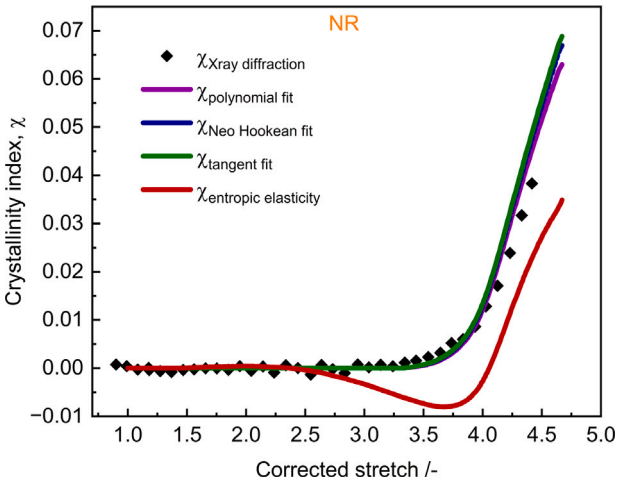

Fig. 7. Crystallinity versus corrected stretch for unfilled NR.

however is not proportional to the stretch rate and cannot therefore be used if the stretch rate is not constant.

Remark 2:. The elastic coupling in unfilled NR is generally considered to be purely entropic. Therefore, in the case of purely entropic elasticity, the strain power density and the heat source superimpose on each other. If the crystallisation does not affect the entropic coupling, it could be assumed that the calorimetric response due to entropic coupling can be identified simply as the strain energy density even if the material is crystallising. This hypothesis is discussed again in subsequent sections and it is the reason why the strain power density is plotted in this figure. The curves of the tangent and the Neo-Hookean-like predictions are quite similar while the curve of the third order polynomial is slightly higher. The strain power density fits the measured heat source quite well for small stretches, typically below 2.5 which corresponds to a time below 340 s in the figure. The strain power density however becomes higher than the measured heat source until the onset of crystallisation. This suggests that non-entropic effects exist, which lead to heat absorption. This demonstrates that significant energetic effects take place before chains start crystallising. As chains significantly orientate before crystallising, the energetic effects could be attributed to chain orientation. For high stretches, the strain power density curve is higher than the predicted heat source curves. The areas between the measured heat source and all the predicted heat sources was determined and used to calculate the crystallinity based on each of the predictions. The crystallinity curves are plotted as a function of stretch in Fig. 7.

The crystallinity obtained from the tangent and the Neo-Hookean-like predictions are in very good agreement with the XRD measurement (represented by the diamond symbols in the figure). The crystallinity obtained for the third order polynomial is slightly lower. The strain power density, which assumes that the elastic coupling is mainly entropic, underestimates the crystallinity and in fact predicts an unrealistic negative crystallinity index at onset.

Remark 3:. The shape of the exothermal peak of crystallisation calculated from the third order polynomial does not show an inflexion for the unfilled NR compound. This is not the case for the CB reinforced NR compounds where there is an inflexion (peak) as detailed in the subsequent sections. Therefore, the prediction of the heat source in the case where there are only elastic couplings does not significantly depend on the chosen expression (the type and order of the polynomial).

From Fig. 7, it has been shown again that the crystallinity results using the surface calorimetric approach are quite similar to that measured by XRD for an unfilled NR compound. The surface calorimetry methodology is next applied to the R2000 CB reinforced NR compound to determine if the technique can be applied to CB reinforced NR compounds as well.

Fig. 8 shows the nominal stress as a function of the measured stretch for the R1200 CB reinforced NR compound (top graph). This particular CB reinforced NR compound is shown here to highlight several interesting features of the stress–strain curves and the calorimetric experiments with materials that have reinforcing fillers. The inclusion of CB as a filler causes significant stress softening and residual strain. For the experiments, the stretch was measured from the displacement of the crosshead and not using non-contact techniques. The initial length is recalculated for each cycle from the residual stretch observed in the previous cycle. Therefore, even in cases where there is slight slip of the test piece in the sample grips (as highlighted by the red circle on the graph), there is no resulting error induced in the stretch calculation. The target stretch and the corrected stretch (for the fifth cycle of each set) are presented in Fig. 8 (bottom graph). The differences in the target stretch and corrected stretch is mainly due to the large residual stretch observed in the CB reinforced compounds. It should be noted that slipping, if any, typically occurs during the first cycle at a specific strain amplitude when the stretch exceeds the maximum stretch previously reached. The fact that the permanent stretch was taken into account for the stretch calculation is absolutely essential when comparing the crystallinity measurement obtained from independent surface calorimetry and XRD techniques.

Fig. 9 shows the nominal stress as a function of the corrected stretch for the last mechanical cycle of the R2000 CB reinforced compound. Compared to the unfilled NR compound, the addition of fillers significantly increases the stiffness of the material and a sharp increase in the stiffening is observed at higher stretch values due to finite extensibility and SIC effects.

The measured temperature variation of the R2000 CB reinforced NR compound is shown as the solid black line in Fig. 10. The temperature typically increases the most on the first cycle at any specific target strain due to Mullins effect. The mean temperature variation slightly decreases within each subsequent cycle at a given strain and eventually stabilises. As was previously done for the unfilled NR compound, the corresponding adiabatic temperature variation is plotted as the dashed black line. At each cycle of a given stretch, the minimum adiabatic temperature variation increases with relatively similar values, except for the first cycle where a higher heat amount is produced due to the Mullins effect. The higher the maximum stretch applied, the higher the

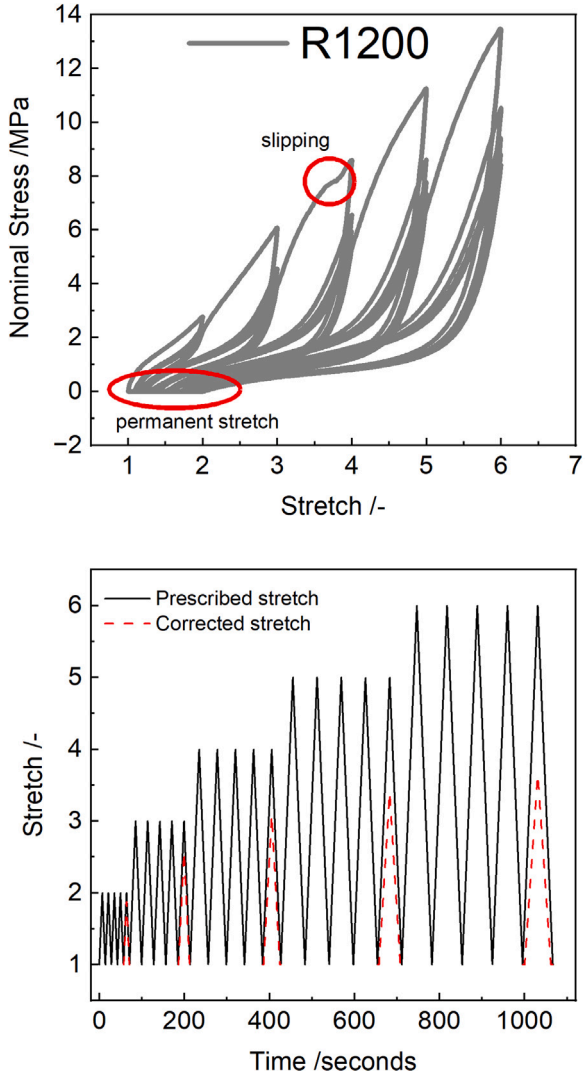

Fig. 8. Nominal stress versus target stretch for R1200 CB reinforced NR compound (top) and targeted and corrected stretches as functions of time (bottom).

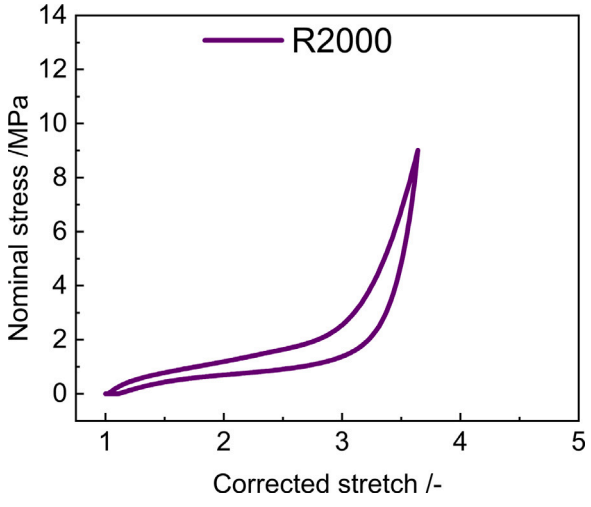

Fig. 9. Nominal stress versus corrected stretch for the last mechanical cycle for R2000 CB reinforced NR compound.

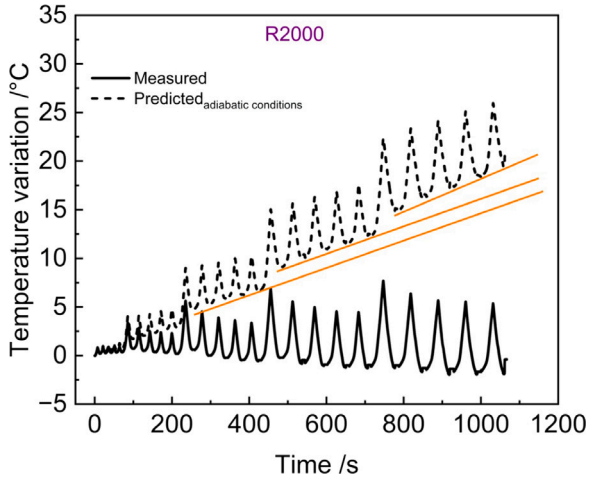

Fig. 10. Temperature variation versus time for the last mechanical cycle for R2000 CB reinforced NR compound.

slope of the line joining the minimum temperature variations, shown as the orange lines in the figure. This suggests higher intrinsic dissipation is produced over each cycle with increasing stretch.

Fig. 11 shows the power densities. The power densities refer to both the heat power density determined from the temperature measurements and the strain power density obtained from the stress tensor and strain rate. The measured heat sources (solid black line) and predicted heat sources (dashed lines) during the fifth cycle for the R2000 CB reinforced NR compound are plotted in Fig. 11. The heat source predictions have been fitted before crystallisation using a Neo-Hookean model, a tangent and a third order polynomial function similar to what was done for the unfilled NR compound. The strain power density has also been plotted. Similar to the unfilled NR compound, the tangent and the Neo-Hookean-like functions provide very good predictions. The prediction using the third order polynomial however differs significantly from what was previously seen in the unfilled NR compound. As the heat source in the reinforced NR compound exhibits a larger exothermal peak at a lower amplitude than the unfilled NR compound, the order of the polynomial chosen for predicting the heat source without crystallisation strongly affects the calculated thermal energy of crystallisation (the area between measured and predicted heat sources) and therefore the crystallinity calculation. The larger exothermal peak occurs for reinforced compounds due to strain amplification effects from the fillers which decreases the global stretch at which crystallisation starts and therefore increases the range over which the exothermal peak occurs. Specifically, predicting the crystallinity using a third order polynomial leads to a much smaller crystallinity than with a Neo-Hookean form. Extending the surface calorimetry technique to reinforced NRs therefore is dependent on choosing an appropriate predicted heat source function. The XRD measurement is utilised in this study to determine the appropriate predicted heat source function. The strain power density is also plotted on the graph. The strain power density shows higher values than the heat source for the entire stretch range prior to the onset of crystallisation. This suggests the inclusion of fillers increases non-entropic effects. Fig. 12 shows the SIC predictions compared to the crystallinity measured using the XRD technique (in black diamond symbols). The tangent and the Neo-Hookean-like predictions provide comparable results to the XRD measurements. The crystallinity curves from the tangent and Neo-Hookean-like predictions superimpose well with each other. The tangent crystallinity curve is shown as a dashed line to make the Neo-Hookean crystallinity curve visible. Both the tangent and Neo-Hookean-like crystallinity curves also superimpose well with the XRD results. The crystallinity curves of the third order

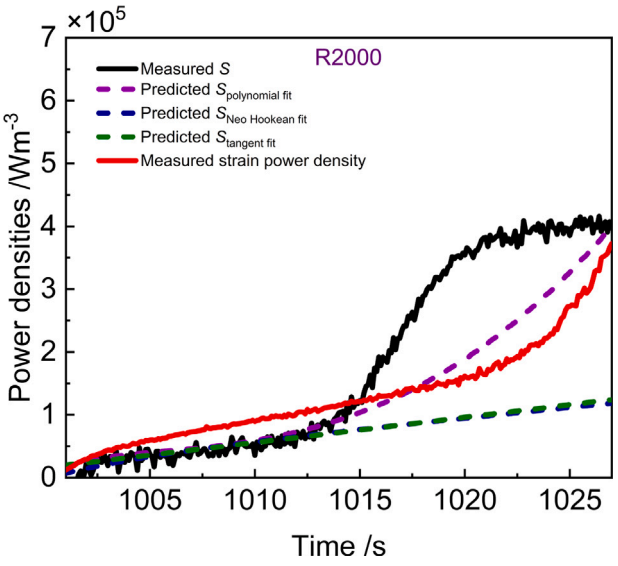

Fig. 11. Power densities versus time for the last mechanical cycle for R2000 CB reinforced NR compound.

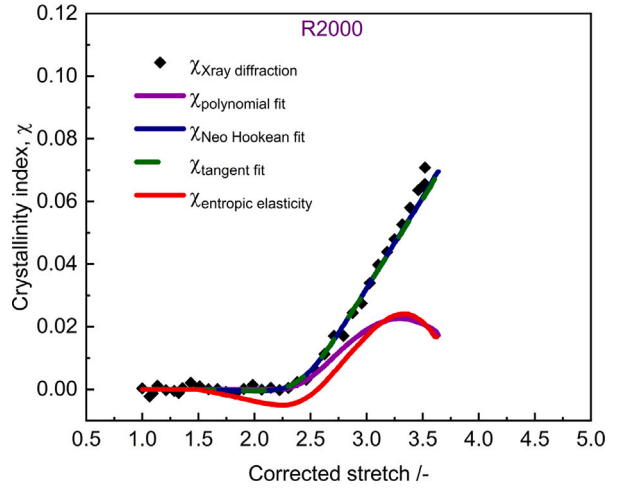

Fig. 12. Crystallinity versus stretch for the last mechanical cycle for R2000 CB reinforced NR compound.

polynomial and the strain power density, however, show poor correlation to the XRD measurement. The two curves show an inflexion as the stretch increases. Based on these observations, the Neo-Hookean-like function is chosen as the appropriate function for generalising the surface calorimetry method to predict the amount of crystallisation in reinforced NR compounds. To validate this approach of applying calorimetric measurements to calculate the extent of crystallisation, two other CB reinforced NR compounds (R1200 and N326) were also analysed. The tangent form was not considered as it does not account for changes in the stretch rate as previously mentioned.

4.2. Validation of the methodology with two different fillers

To validate the methodology proposed for using surface calorimetry for reinforced NR compounds, the crystallinity measured using this approach in the two other CB reinforced NR compounds (R1200 and N326) was compared with the XRD measurements made under broadly comparable testing conditions. The nominal stress versus the corrected stretch is presented in Fig. 13(a) and Fig. 13(b) for the R1200 compound and the N326 compound respectively. As previously mentioned, the different types of fillers influence the mechanical response of the compounds, and therefore the crystallisation. The temperature variation in the two CB reinforced NR compounds is shown in Fig. 14. The heat diffusion equation is used to determine the calorimetric responses and plotted in Fig. 15. The heat sources have been fitted prior to crystallisation using a Neo-Hookean like function (shown in blue dashed lines).

The crystallinity of the compounds is calculated and the crystallinity curves plotted in Fig. 16 as the blue solid line. The crystallinity measured using the XRD technique is plotted using the black diamond symbols. Fig. 16 shows that the crystallinity obtained using the surface calorimetry technique provides comparable values to the crystallinity obtained using the XRD technique. The repeatability of the methodology indicates that using the Neo-Hookean-like function to analyse the surface temperature enables the new approach of accurately estimating the SIC in CB reinforced elastomers to work.

5. Conclusion

In this paper, the surface calorimetry approach initially developed to determine the crystallinity of unfilled NR compounds has been extended to reinforced NR compounds. Three CB reinforced NR compounds were used. The CBs had similar loading of 50 phr in the compounds but varied in their surface area and structure which imparted different mechanical properties on the resulting compounds. An unfilled equivalent was included as well. The crystallinity of the compounds was measured using the classical XRD measurements. As a first step, the relevance of the calorimetric technique for determining the crystallinity in an unfilled NR was confirmed by comparing the crystallinity obtained from surface calorimetry and XRD techniques. To extend the surface calorimetry technique to CB reinforced NR compounds, an identification procedure to determine the thermal energy of crystallisation was developed. This identification technique was determined by comparing the crystallinity obtained from the surface calorimetry with the crystallinity obtained from XRD measurements. This methodology entails fitting a Neo-Hookean-like function to the calorimetric response prior to the onset of crystallisation. The methodology was validated by applying it to two other NR compounds reinforced with different types of CB. The results show satisfactory correlation with the crystallinity obtained from XRD measurements and thus extends and validates the calorimetric technique to enable the determination of SIC in CB reinforced NR compounds. Extending the calorimetric approach to determine the SIC of CB reinforced NR compounds has quite useful implications. While the proposed surface calorimetry technique is not intended to replace the classical XRD technique, since it does not provide details such as the crystalline phase structure, chain orientation and kinetics of crystallisation, it is a relatively accessible methodology that does not require a complex set up and thus can be used for evaluating the level of crystallinity during deformation in a CB reinforced rubber compound. It can therefore be easily used for evaluating CB reinforced rubber compounds during compound development for engineering. For example, the calorimetric approach does not require the measurement of the mechanical response (the stress versus stretch) during the test. It is therefore convenient for crystallinity measurements in the presence of stress gradients, typically at crack tips, where estimating the mechanical response is complicated or impossible.

CRediT authorship contribution statement

Jean-Benoit Le Cam: Writing – original draft, Validation, Supervision, Resources, Project administration, Methodology, Investigation, Formal analysis, Conceptualization. **William Amoako Kyei-Manu:** Writing – review & editing, Visualization, Validation, Methodology, Investigation, Formal analysis, Data curation. **Adel Tayeb:** Writing –

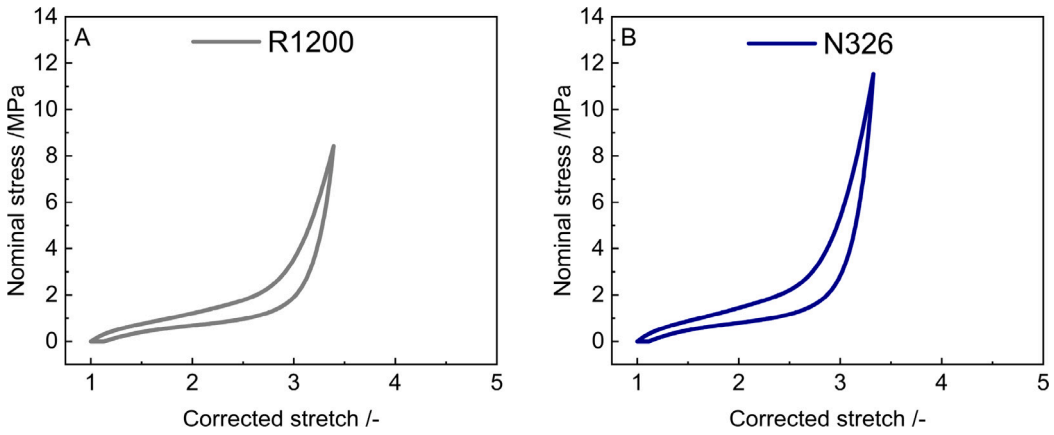

Fig. 13. Nominal stress versus corrected stretch for the last mechanical cycle (a) R1200 CB compound (b) N326 CB compound.

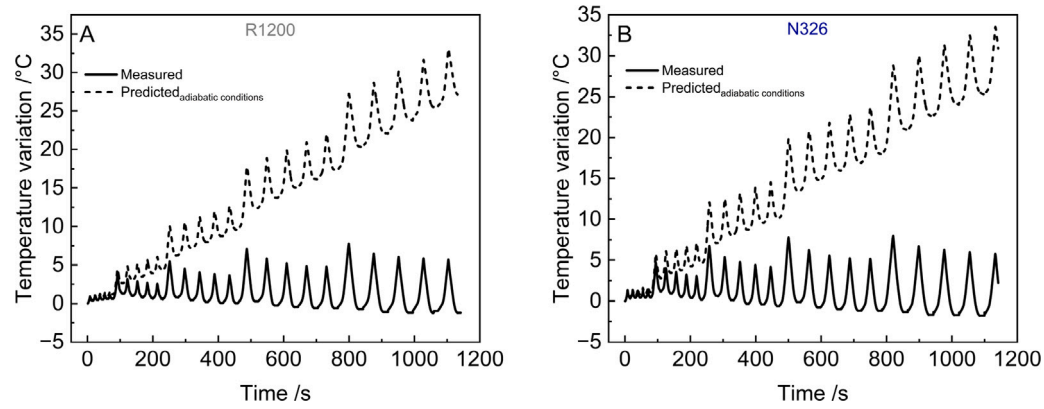

Fig. 14. Temperature variation versus time for the last mechanical cycle of (a) R1200 CB compound (b) N326 CB compound.

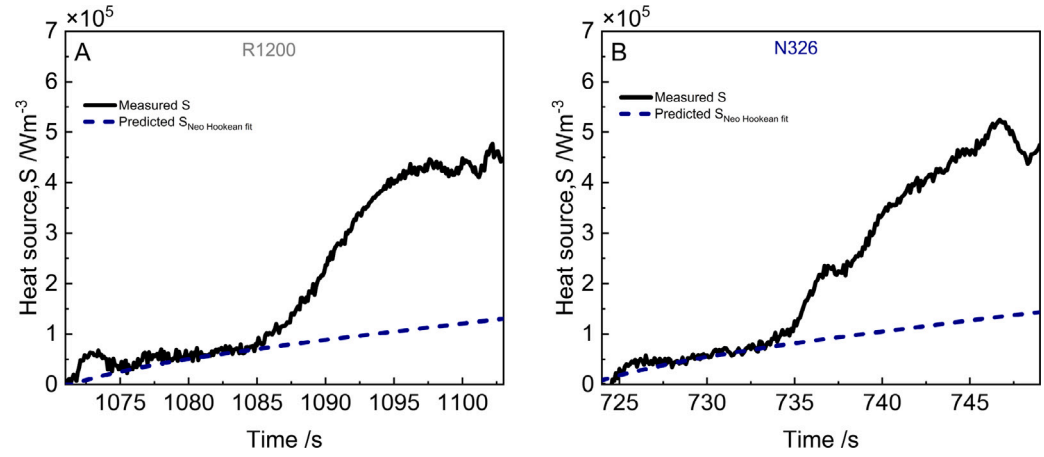

Fig. 15. Heat source versus time for the last mechanical cycle of (a) R1200 CB compound (b) N326 CB compound.

review & editing, Validation, Methodology, Formal analysis, Data curation. **Pierre-Antoine Albouy:** Writing – review & editing, Validation, Methodology, Investigation, Formal analysis. **James J.C. Busfield:** Writing – review & editing, Validation, Supervision, Resources, Project administration, Funding acquisition, Conceptualization.

Declaration of competing interest

The authors declare the following financial interests/personal relationships which may be considered as potential competing interests: William Amoako Kyei-Manu reports financial support and equipment, drugs, or supplies were provided by Birla Carbon USA Inc., Marietta, GA, USA.

Data availability

Data will be made available on request.

Acknowledgements

The authors would like to thank Birla Carbon for funding and providing materials for this research.

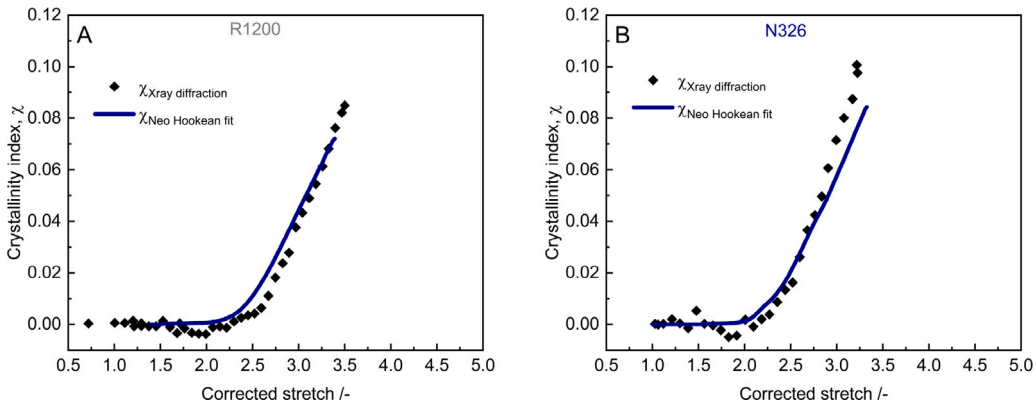

Fig. 16. Crystallinity versus corrected stretch for the fifth mechanical cycle at the largest strain for with (a) R1200 CB compound (b) N326 CB compound.

Funding

This research was funded by Birla Carbon USA Inc., Marietta, GA, USA.

Appendix A. Supplementary data

Supplementary material related to this article can be found online at https://doi.org/10.1016/j.polymertesting.2024.108341.

References

[1] H. Feuchter, The volume contraction with the formation of anisotropic rubber systems by stretching, Gummi-Ztg 39 (1925) 1167–1168.
[2] J. Katz, Nature 4 (169) (1925).
[3] S.M. Cadwell, R.A. Merril, C.M. Sloman, F.L. Yost, Dynamic fatigue life of rubber, Ind. Eng. Chem. (reprinted in Rubber Chem. and Tech. 13 (1940) 304-315) 12 (1940) 19–23.
[4] J.H. Fielding, Flex life and crystallisation of synthetic rubber, Ind. Eng. Chem. 35 (1943) 1259–1261.
[5] J.R. Beatty, Fatigue of rubber, Rubber Chem. Technol. 37 (1964) 1341–1364.
[6] C. Bunn, Molecular structure and rubber-like elasticity I. The crytsal structures of Beta gutta-percha, rubber and polychloroprene, Proc. R. Soc. London, Ser. 1 180 (1942) 40.
[7] Y. Takahashi, T. Kumano, Crystal structure of natural rubber, Macromolecules 37 (4860) (2004).
[8] A. Immirzi, C. Tedesco, G. Monaco, A. Tonelli, Crystal structure and melting entropy of natural rubber, Macromolecules 38 (1223) (2005).
[9] G. Rajkumar, J. Squire, S. Arnott, Macromolecules 39 (7004) (2006).
[10] S. Toki, I. Sics, S. Ran, L. Liu, B. Hsiao, S. Murakami, M. Tosaka, S. Kohjiya, S. Poompradub, Y. Ikeda, A. Tsou, Rubber Chem. Technol. 42 (2004) 956–964.
[11] S. Toki, T. Fujimaki, M. Okuyama, Strain-induced crystallization of natural rubber as detected real-time by wide-angle x-ray diffraction technique, Polymer 41 (2000) 5423–5429.
[12] S. Trabelsi, P.-A. Albouy, J. Rault, Effective local deformation in stretched filled rubber, Macromolecules 36 (2003b) 9093–9099.
[13] K. Brüning, K. Schneider, S.V. Roth, G. Heinrich, Strain-induced crystallization around a crack tip in natural rubber under dynamic load, Polymer 54 (2013b) 6200–6205.
[14] P. Rublon, B. Huneau, E. Verron, N. Saintier, S. Beurrot, L, A, C. Mocuta, D. Thiaudière, D. Berghezan, Multiaxial deformation and strain-induced crystallization around a fatigue crack in natural rubber, Eng. Fract. Mech. 123 (2014) 59–69.
[15] J.C. Mitchell, D.J. Meier, Rapid stress-induced crystallization in natural rubber, J. Polym. Sci. A-2: Polym. Phys. 6 (1968) 1689–1703.
[16] N. Candau, R. Laghmach, L. Chazeau, J.-M. Chenal, C. Gauthier, T. Biben, E. Munch, Influence of strain rate and temperature on the onset of strain induced crystallization in natural rubber, Eur. Polym. J. 64 (2015) 244–252.
[17] J. Plagge, M. Klüppel, Determining strain-induced crystallization of natural rubber composites by combined thermography and stress–strain measurements, Polym. Test. 66 (2018) 87–93.
[18] J.-B. Le Cam, Strain-induced crystallization in rubber: A new measurement technique, Strain 54 (2018) e12256.
[19] J.-B. Le Cam, P.-A. Albouy, S. Charlès, Comparison between x-ray diffraction and quantitative surface calorimetry based on ir thermography to evaluate strain-induced crystallinity in natural rubber, Rev. Sci. Instrum. 91 (2020) 044902.
[20] J.R. Samaca Martinez, J.-B. Le Cam, X. Balandraud, E. Toussaint, J. Caillard, Filler effects on the thermomechanical response of stretched rubbers, Polym. Test. 32 (2013a) 835–841.
[21] J.R. Samaca Martinez, J.-B. Le Cam, X. Balandraud, E. Toussaint, J. Caillard, New elements concerning the Mullins effect: A thermomechanical analysis, Eur. Polym. J. 55 (2014) 98–107.
[22] J.-B. Le Cam, J.Samaca. Martinez, X. Balandraud, E. Toussaint, J. Caillard, Thermomechanical analysis of the singular behavior of rubber: Entropic elasticity, reinforcement by fillers, strain-induced crystallization and the mullins effect, Exper. Mech. 55 (2015) 771–782.
[23] M. Loukil, G. Corvec, E. Robin, M. Miroir, J.-B. Le Cam, P. Garnier, Stored energy accompanying cyclic deformation of filled rubber, Eur. Polym. J. 98 (2018) 448–455.
[24] V.N. Khiem, J.-B. Le Cam, S. Charlès, M. Itskov, Thermodynamics of strain-induced crystallization in filled natural rubber under uni- and biaxial loadings. Part I: Complete energetic characterization and crystallinity evaluation, J. Mech. Phys. Solids 159 (2022a) 104701.
[25] P.-A. Albouy, A. Vieyres, R. Perez-Aparicio, O. Sanseau, P. Sotta, The impact of strain-induced crystallization on strain during mechanical cycling of cross-linked natural rubber, Polymer 55 (2014) 4022–4031.
[26] P.-A. Albouy, P. Sotta, Draw ratio at the onset of strain-induced crystallization in cross-linked natural rubber, Macromolecules 53 (2020) 992–1000.
[27] S. Trabelsi, P. Albouy, J. Rault, Crystallization and melting processes in vulcanized stretched natural rubber, Macromolecules 36 (2003a) 7624–7639.
[28] S. Trabelsi, P.-A. Albouy, J. Rault, Stress induced crystallizatiion of natural and synthetic poly cis isoprene, Rubber Chem. Technol. 77 (2004) 303–316.
[29] H. Louche, Etudes De Certains Phénomènes De Localisation À Partir De Champs Thermomécaniques Habilitation thesis, Savoie University, 2009.
[30] S. Charlès, J.-B. Le Cam, Inverse identification from heat source fields: a local approach applied to hyperelasticity, Strain 56 (2020) e12334.
[31] A. Chrysochoos, Analyse du comportement des matériaux par thermographie infra rouge, in: Colloque Photomécanique, Vol. 95, 1995, pp. 201–211.
[32] A. Chrysochoos, H. Louche, An infrared image processing to analyse the calorific effects accompanying strain localisation, Int. J. Eng. Sci. 38 (2000) 1759–1788.
[33] J.R. Samaca Martinez, J.-B. Le Cam, X. Balandraud, E. Toussaint, J. Caillard, Thermal and calorimetric effects accompanying the deformation of natural rubber. Part 2: quantitative calorimetric analysis, Polymer 54 (2013b) 2727–2736.
[34] T. Spratte, J. Plagge, M. Wunde, M. Klüppel, Investigation of strain-induced crystallization of carbon black and silica filled natural rubber composites based on mechanical and temperature measurements, Polymer 115 (2017) 12–20.
[35] D. Göritz, F.H. Müller, Die kalorimetrische erfassung der dehnungskristallisation polymerer, Kolloid-Z. Z. Polymere 241 (1970) 1075–1079.
[36] K. Brüning, K. Schneider, S.V. Roth, G. Heinrich, Kinetics of strain-induced crystallization in natural rubber studied by waxd: Dynamic and impact tensile experiments, Macromolecules 45 (2012) 7914–7919.
[37] K. Brüning, K. Schneider, G. Heinrich, In-Situ Structural Characterization of Rubber during Deformation and Fracture, Springer, Berlin, Heidelberg, 2013a, pp. 43–80.
[38] K. Brüning, K. Schneider, S.V. Roth, G. Heinrich, Kinetics of strain-induced crystallization in natural rubber: A diffusion-controlled rate law, Polymer 72 (2015) 52–58, Macromolecular Engineering - Dedicated to Professor Krzysztof Matyjaszewski on the Occasion of his 65th Birthday.
[39] L.R.G. Treloar, The elasticity and related properties of rubbers, Rep. Progr. Phys. 36 (755) (1973).
[40] J.-B. Le Cam, Energy storage due to strain-induced crystallization in natural rubber: the physical origin of the mechanical hysteresis, Polymer 127 (2017) 166–173.

[41] V.N. Khiem, J.-B. Le Cam, S. Charlès, M. Itskov, Thermodynamics of strain-induced crystallization in filled natural rubber under uni- and biaxial loadings. Part II: Physically-based constitutive theory, J. Mech. Phys. Solids 159 (2022b) 104712.

[42] V. Honorat, S. Moreau, J. Muracciole, B. Wattrisse, A. Chrysochoos, Calorimetric analysis of polymer behaviour using a pixel calibration of an irfpa camera, Quant. Infrared Thermogr. 2 (2005) 189–200.

[43] R. Caborgan, Contribution À L'analyse Expérimentale Du Comportement Thermomécanique Du Caoutchouc Naturel Thèse de doctorat Montpellier 2, (Ph.D. thesis), 2011.

[44] W.A. Kyei-Manu, C.R. Herd, M. Chowdhury, J.J.C. Busfield, L.B. Tunnicliffe, The influence of colloidal properties of carbon black on static and dynamic mechanical properties of natural rubber, Polymers 14 (2022).

[45] A. Chrysochoos, V. Huon, F. Jourdan, J.-M. Muracciole, R. Peyroux, B. Wattrisse, Use of full-Field digital image correlation and infrared thermography measurements for the thermomechanical analysis of material behaviour, Strain 46 (2010) 117–130.

[46] S. Trabelsi, P.-A. Albouy, J. Rault, Stress-induced crystallization around a crack tip in natural rubber, Macromolecules 35 (2002) 10054–10061.

[47] J. Marchal, Cristallisation Des Caoutchoucs Chargés Et Non Chargés Sous Contrainte : Effet Sur Les Chaînes Amorphes (Ph.D. thesis), Université Paris XI Orsay, France, 2006.

[48] W.A. Kyei-Manu, L.B. Tunnicliffe, J. Plagge, C.R. Herd, K. Akutagawa, N.M. Pugno, J.J.C. Busfield, Thermomechanical characterization of carbon black reinforced rubbers during rapid adiabatic straining, Front. Mater. (2021).

[49] X. Balandraud, J.-B. Le Cam, Some specific features and consequences of the thermal response of rubber under cyclic mechanical loading, Arch. Appl. Mech. 84 (2014) 773–788.